

# On Phase Transition of Compressed Sensing in the Complex Domain

Zai Yang, Cishen Zhang, and Lihua Xie, *Fellow, IEEE*

**Abstract**—The phase transition is a performance measure of the sparsity-undersampling tradeoff in compressed sensing (CS). This letter reports, for the first time, the existence of an exact phase transition for the  $\ell_1$  minimization approach to the complex valued CS problem. This discovery is not only a complementary result to the known phase transition of the real valued CS but also shows considerable superiority of the phase transition of complex valued CS over that of the real valued CS. The results are obtained by extending the recently developed ONE-L1 algorithms to complex valued CS and applying their optimal and iterative solutions to empirically evaluate the phase transition.

**Index Terms**—Compressed sensing, complex signals,  $\ell_1$  minimization, ONE-L1 algorithms, Phase transition.

## I. INTRODUCTION

Compressed sensing (CS) has made significant impact on information theory and signal processing since the pioneering works of Candès *et al.* [1] and Donoho [2]. It aims at reconstructing a signal from reduced number of linear measurements under a sparsity/compressibility condition. Different from the conventional linear reconstruction approach, a nonlinear scheme is used in CS to solve the convex optimization problem

$$(P_1) \quad \min_{\mathbf{x}} \|\mathbf{x}\|_1, \text{ subject to } \mathbf{Ax} = \mathbf{b},$$

where  $\mathbf{x} \in \mathbb{C}^N$  is a sparse signal to be recovered,  $\mathbf{A} \in \mathbb{C}^{n \times N}$  is a sensing matrix and  $\mathbf{b} \in \mathbb{C}^n$  is a vector of sample data, with  $N$  and  $n$  being the signal length and sample size respectively and typically  $n \ll N$ .

The theory of CS is mainly focused on studying how aggressively a sparse signal can be undersampled while still preserving all information for its reconstruction. Existing undersampling theories include those based on incoherence [3] and restricted isometry property (RIP) [4], and phase transition theory [5]. While the incoherence and RIP are sufficient conditions for sparse signal reconstruction and typically quite conservative in practice [6], the phase transition is most precise owing to its necessary and sufficient condition. Given the real signal  $\mathbf{x}$  and sensing matrix  $\mathbf{A}$  with i.i.d. random Gaussian entries, it asserts that the behavior of the sparsity-undersampling tradeoff of  $(P_1)$  is precisely controlled by the sampling ratio  $\delta = n/N$  and sparsity ratio  $\rho = k/N$ , where  $k$  denotes the number of nonzero entries of  $\mathbf{x}$ . Accordingly, there exists a transition curve in the phase plane of  $(\delta, \rho)$

Z. Yang and L. Xie are with the School of Electrical and Electronic Engineering, Nanyang Technological University, 639798, Singapore (e-mail: yang0248@ntu.edu.sg; elhxie@ntu.edu.sg).

C. Zhang is with the Faculty of Engineering and Industrial Sciences, Swinburne University of Technology, Hawthorn VIC 3122, Australia (e-mail: cishenzhang@swin.edu.au).

This work has been submitted to IEEE Signal Processing Letters for possible publication.

under which a successful reconstruction can be achieved with an overwhelming probability. Moreover, an expression of the transition curve has also been obtained [5].

To the best of our knowledge, so far the results on phase transition only deal with real signals. This letter is the first work studying the phase transition of CS in the more general complex domain. The significance of our work is twofold: 1) discovering a new and exact phase transition of complex valued CS so to inspire completeness of the phase transition theory; 2) providing insight into performance of numerous CS applications involving complex data, e.g., magnetic resonance imaging (MRI) [7], radar imaging [8] and source localization [9].

This letter shows that the recently developed orthonormal expansion  $\ell_1$ -minimization (ONE-L1) algorithms [10] for CS can be extended to the complex case after some modifications. The algorithms can compute the optimal solution of  $(P_1)$  with low computational complexities so to provide an effective means for empirically exploring the sparsity-undersampling tradeoff of complex valued CS. A remarkable finding is that, not only a transition curve exists in the phase plane of complex CS, but also it is well above that of the real valued CS. It therefore displays a significantly enlarged region of success in the phase transition plane. Moreover, the universality of phase transitions across many different matrix ensembles [11] also holds in the complex case.

In this letter, Section II retrospect the main points in [10] on ONE-L1 algorithms and extends the algorithms to the complex CS. Section III applies the extended ONE-L1 algorithms to explore the phase transition of complex CS. Conclusion is drawn in Section IV.

## II. ONE-L1 ALGORITHMS FOR COMPLEX SIGNALS

The ONE-L1 algorithms in [10] solve the  $\ell_1$  minimization problem  $(P_1)$  for real  $\mathbf{x}$ ,  $\mathbf{A}$  and  $\mathbf{b}$ . Assume that the sensing matrix  $\mathbf{A}$  is partially orthonormal, i.e.,  $\mathbf{A}\mathbf{A}' = \mathbf{I}$  with  $'$  denoting the transpose and  $\mathbf{I}$  an identity matrix, and let  $\Gamma(\mathbf{d})$  be an operator projecting the vector  $\mathbf{d}$  onto its first  $n$  entries. The orthonormal expansion technique is to introduce an expanded orthonormal matrix  $\Phi$  to reformulate the optimization problem  $(P_1)$  into

$$(P_1^o) \quad \begin{aligned} & \min_{(\mathbf{x}, \mathbf{d})} \|\mathbf{x}\|_1 \\ & \text{subject to } \Phi\mathbf{x} = \mathbf{d} \text{ and } \Gamma(\mathbf{d}) = \mathbf{b}, \end{aligned}$$

where the first  $n$  rows of  $\Phi$  compose  $\mathbf{A}$  and the rest orthonormal  $N - n$  rows are arbitrary.

The augmented Lagrange multiplier (ALM) method is applied in [10] to  $(P_1^o)$  and the obtained result leads to an exact ONE-L1 (eONE-L1) algorithm for iterative computation of the optimal solution. While eONE-L1 has an inner iteration

loop embedded in the outer loop iteration, its relaxed version, rONE-L1, further speeds up the computation by simplifying the inner loop iteration into a single update. The rONE-L1 algorithm is numerically optimal in terms of the sparsity-undersampling tradeoff under reasonable parameter settings, i.e., its phase transition result matches that of  $(P_1)$ . It has been shown that rONE-L1 is of iterative thresholding type and is very fast, with appropriate settings of the regulation variable, in comparison with other state-of-the-art algorithms.

An important operation in ONE-L1 algorithms is the soft thresholding defined as

$$S_\epsilon(w) = \operatorname{sgn}(w) \cdot (|w| - \epsilon)^+,$$

for  $w \in \mathbb{R}$ , where  $\epsilon \in \mathbb{R}_+$ ,  $(\cdot)^+ = \max(\cdot, 0)$  and

$$\operatorname{sgn}(w) = \begin{cases} w/|w|, & w \neq 0; \\ 0, & w = 0. \end{cases}$$

In fact,  $S_\epsilon(\mathbf{w})$  operates elementwisely on a real valued vector  $\mathbf{w}$ . It has been well known that the soft thresholding solves the following  $\ell_1$  regularized least squares problem

$$S_\epsilon(\mathbf{w}) = \arg \min_{\mathbf{v}} \left\{ \epsilon \|\mathbf{v}\|_1 + \frac{1}{2} \|\mathbf{w} - \mathbf{v}\|_2^2 \right\} \quad (1)$$

for real valued vectors  $\mathbf{w}, \mathbf{v}$  of the same dimension.

To extend the ONE-L1 algorithms to the complex case, the complex sensing matrix  $\mathbf{A} \in \mathbb{C}^{n \times N}$  is also assumed to satisfy  $\mathbf{A}\mathbf{A}' = \mathbf{I}$  with  $'$  denoting the conjugate transpose. The soft thresholding operator  $S_\epsilon(\mathbf{w})$ , for a complex vector  $\mathbf{w}$ , is defined as in the real case. It is also the optimal solution to (1) for complex valued vectors  $\mathbf{w}, \mathbf{v}$ . Let  $\Re$  and  $\Im$  be operators taking, respectively, the real and imaginary part of a variable. The augmented Lagrangian function in [10] is modified, for the complex CS problem, as

$$\mathcal{L}(\mathbf{x}, \mathbf{d}, \mathbf{y}, \mu) = \|\mathbf{x}\|_1 + \Re \langle \mathbf{d} - \Phi \mathbf{x}, \mathbf{y} \rangle + \frac{\mu}{2} \|\mathbf{d} - \Phi \mathbf{x}\|_2^2,$$

where  $\mathbf{y} \in \mathbb{C}^N$  is the Lagrange multiplier vector,  $\mu \in \mathbb{R}_+$  is a regulation parameter and  $\langle \mathbf{u}_1, \mathbf{u}_2 \rangle = \mathbf{u}_1' \mathbf{u}_2 \in \mathbb{C}$  is the inner product of  $\mathbf{u}_1, \mathbf{u}_2 \in \mathbb{C}^N$ . The modified augmented Lagrangian function allows a straightforward extension of the derivation and optimization steps in [10] to the complex CS problem  $(P_1)$ , yielding the optimal solution in the same form as that of the real valued CS. As a result, the ONE-L1 algorithms as given in [10] can be directly applicable to the complex CS problem. Readers are referred to [10] for detailed algorithm steps and the optimality and convergence analysis.

### III. PHASE TRANSITION OF COMPLEX CS

#### A. The Phase Transition Problem of Complex CS

The phase transition measures the sparsity-undersampling tradeoff performance and is defined for the signal length  $N \rightarrow \infty$  in the CS theory [5]. For a real signal  $\mathbf{x}$  and a sensing matrix  $\mathbf{A}$  with i.i.d. random Gaussian entries, the sparsity-undersampling tradeoff of  $(P_1)$  is controlled by the sampling ratio  $\delta$  and sparsity ratio  $\rho$ . As a result, the plane of  $(\delta, \rho)$  is divided by a phase transition curve into two phases, a ‘success’ phase where  $(P_1)$  successfully recovers the sparse signal and

a ‘failure’ phase where the original signal cannot be recovered by solving  $(P_1)$ , both with an overwhelming probability.

For real  $\mathbf{x}$  and  $\mathbf{A}$ , three different approaches, including combinatorial geometry [5], null space method [12] and state evolution [13], have been used to derive the phase transition of  $(P_1)$  and their results agree with each other. Numerical simulations have shown that the observed phase transition matches the theoretical curve even for modestly large  $N$ , e.g.,  $N = 1000$  [10], [11], where the phase transition for finite- $N$  is defined as the value of  $\rho$  at which the original signal is successfully reconstructed with a probability of 50%. Moreover, it is observed that the assumption of Gaussianity of  $\mathbf{A}$  can be relaxed in practice, known as the universality of phase transitions [11].

If  $\mathbf{x}$  is a complex signal, a popularly known and simple treatment is to transform it into the real  $\begin{bmatrix} \Re \mathbf{x} \\ \Im \mathbf{x} \end{bmatrix}$  followed by solving the resulting real CS problem [14], [15]

$$(P_1^I) \quad \begin{aligned} & \min_{\mathbf{x}} \|\Re \mathbf{x}\|_1 + \|\Im \mathbf{x}\|_1, \\ & \text{subject to } \begin{bmatrix} \Re \mathbf{A} & -\Im \mathbf{A} \\ \Im \mathbf{A} & \Re \mathbf{A} \end{bmatrix} \cdot \begin{bmatrix} \Re \mathbf{x} \\ \Im \mathbf{x} \end{bmatrix} = \begin{bmatrix} \Re \mathbf{b} \\ \Im \mathbf{b} \end{bmatrix}. \end{aligned}$$

By defining  $S_\epsilon^I(\mathbf{w}) = S_\epsilon(\Re \mathbf{w}) + j \cdot S_\epsilon(\Im \mathbf{w})$  with  $j = \sqrt{-1}$ , the problem  $(P_1^I)$  can be solved by ONE-L1 algorithms with  $S_\epsilon(\cdot)$  replaced by  $S_\epsilon^I(\cdot)$ . This formulation of the complex CS problem into  $(P_1^I)$  is thereafter called the indirect method.

So far the existing results on the phase transition are only for real  $\mathbf{x}$  and  $\mathbf{A}$ . The questions about whether there exists a sharp phase transition for complex  $\mathbf{x}$  and  $\mathbf{A}$  and whether it, if exists, is different from that in the real case are still open. In  $(P_1^I)$  with the signal length  $N^I = 2N$ , sample size  $n^I = 2n$  and sparsity level  $k^I = 2k$ , the corresponding sampling ratio  $\delta$  and sparsity ratio  $\rho$  are unchanged, so should be the phase transition, as to be illustrated in the next subsection.

However, the observation that the transformed real CS problem  $(P_1^I)$  has the same phase transition as that of the real valued CS does not sufficiently mean that the original complex CS problem  $(P_1)$  has the same phase transition as that of the real valued CS. It is noted that the reformulation of  $(P_1)$  into  $(P_1^I)$  masks the fact that the objective function of  $(P_1^I)$  is not equivalent to that of  $(P_1)$ . Thus the problems  $(P_1^I)$  and  $(P_1)$  may have different optimal solutions and, hence, different phase transitions.

#### B. ONE-L1 Estimation of Phase Transition of Complex CS

Section II has shown that the ONE-L1 algorithms can be extended and applicable to the complex valued CS problem. The eONE-L1 achieves the optimal solution of  $(P_1)$  and rONE-L1 is numerically optimal and exponentially converges, which are applied in this subsection to empirically explore the sparsity-undersampling tradeoff of  $(P_1)$ . The implementations of ONE-L1 algorithms follow the same procedure as their real versions in [10]. We fix  $r > 1$  and let  $\mu_{t+1} = r \cdot \mu_t$ . The parameter  $r$  is set to  $r = 1 + \delta$  in eONE-L1 and  $r = \min(1 + 0.04\delta, 1.02)$  is chosen in rONE-L1. The success of recovering the original signal is stated if the relative root mean squared error (RRMSE)  $\|\hat{\mathbf{x}} - \mathbf{x}^o\|_2 / \|\mathbf{x}^o\|_2 < 10^{-4}$ ,

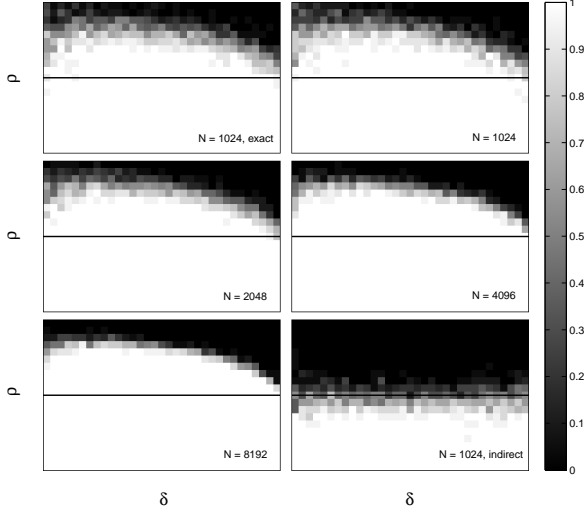


Fig. 1. Observed success rates of partial-Fourier sampling. Six images show results of eONE-L1 with signal length  $N = 1024$ , rONE-L1 with  $N = 1024$ , 2048, 4096 and 8192 and the indirect method with  $N = 1024$ , respectively. In each image, every pixel refers to one success rate  $S/M$  with respect to  $(\delta, \rho)$ . The sampling ratio  $\delta$  ranges from 0.02 (left) to 0.98 (right) with an interval 0.03; the sparsity ratio  $\rho$  is from  $\rho^R(\delta) - 0.1$  (bottom) to  $\rho^R(\delta) + 0.1$  (top) with an interval 0.01 with respect to each  $\delta$  (only the middle half of experiment results is shown). The middle line in each image refers to the real phase transition  $\rho^R(\delta)$  of  $(P_1)$ .

where  $\mathbf{x}^o$  and  $\hat{\mathbf{x}}$  are the original and recovered signals, respectively. Meanwhile, the failure to solve  $(P_1)$  using ONE-L1 algorithms is stated if  $\|\hat{\mathbf{x}}\|_1 \geq (1 + 10^{-5}) \|\mathbf{x}^o\|_1$  and  $\|\hat{\mathbf{x}} - \mathbf{x}^o\|_2 / \|\mathbf{x}^o\|_2 \geq 10^{-4}$ , and the failure to solve  $(P_1^I)$  if  $\|\Re \hat{\mathbf{x}}\|_1 + \|\Im \hat{\mathbf{x}}\|_1 \geq (1 + 10^{-5}) (\|\Re \mathbf{x}^o\|_1 + \|\Im \mathbf{x}^o\|_1)$  and  $\|\hat{\mathbf{x}} - \mathbf{x}^o\|_2 / \|\mathbf{x}^o\|_2 \geq 10^{-4}$ .

Inspired by the estimation of the real phase transition in [10], [11], [13], we first set a complex matrix ensemble, e.g., Gaussian, and dimension  $N$ . A grid of  $(\delta, \rho)$  is generated in the plane  $[0, 1] \times [0, 1]$  with equispaced  $\delta \in \{0.02, 0.05, \dots, 0.98\}$  and  $\rho \in \{\rho^R(\delta) + 0.01(i - 21) : i = 1, 2, \dots, 41\}$  with respect to  $\delta$ , where  $\rho^R(\delta)$  denotes the real phase transition. For each combination of  $(\delta, \rho)$ ,  $M = 20$  random problem instances are generated and solved with  $n = \lceil \delta N \rceil$  and  $k = \lceil \rho n \rceil$ . The number of success  $S$  among  $M$  instances is recorded. After data acquisition, a generalized linear modal (GLM) with a logistic link is used to estimate the phase transition as in [10], [13].

We now explore the sparsity-undersampling tradeoffs of  $(P_1)$  and  $(P_1^I)$  with partial-Fourier sampling. Four values of signal length  $N$  are considered, including 1024, 2048, 4096 and 8192. When  $N = 1024$ , both eONE-L1 and rONE-L1 are used to estimate the phase transition of  $(P_1)$ . The rONE-L1 algorithm is used for other  $N$ . Few failures to solve  $(P_1)$  and  $(P_1^I)$  occur when using rONE-L1. See time consumptions and numbers of failures in Table I.

The observed success rates of our experiments are shown in Fig. 1, where the phase-transition performance can be observed. The phase transitions of  $(P_1)$  with complex signals occur at about the same location, higher than that in the

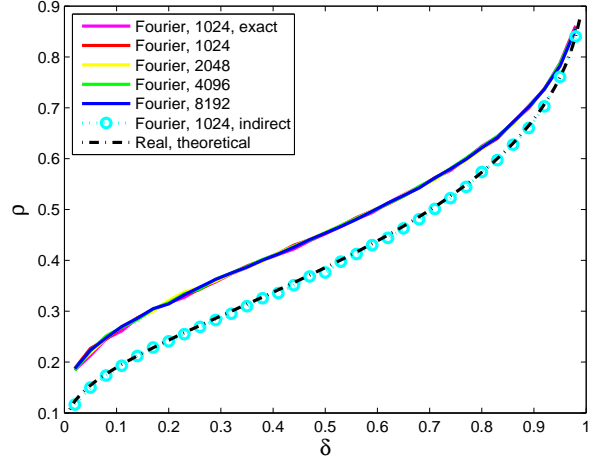


Fig. 2. Observed phase transitions of partial-Fourier sampling. The upper five curves are observed phase transitions estimated by eONE-L1 with  $N = 1024$  and rONE-L1 with  $N = 1024, 2048, 4096$  and 8192, respectively. The lower two are observed phase transitions using the indirect method with  $N = 1024$  and the theoretical real phase transition of  $(P_1)$ . Note that, 1) all observed phase transitions of  $(P_1)$  coincide and are higher than the real phase transition, and 2) the observed phase transition of  $(P_1^I)$  matches the real phase transition.

real case. A larger signal length  $N$  can provide a clearer phase transition, which is consistent with the behavior of the real phase transition of  $(P_1)$  [11]. To the contrary, the phase transition of  $(P_1^I)$  occurs around the real phase transition.

Fig. 2 presents the estimated phase transitions of partial-Fourier sampling. The five observed phase transitions of  $(P_1)$ , estimated respectively by eONE-L1 with  $N = 1024$  and rONE-L1 with  $N = 1024, 2048, 4096$  and 8192, coincide with each other and are higher than the real phase transition of  $(P_1)$ , while the observed phase transition of  $(P_1^I)$  matches the real phase transition.

Based on our experimental results, two findings are stated as follows.

**Finding 1:** For complex signals and the partial-Fourier matrix ensemble with large dimension  $N$ , we observe that

- I. the  $\ell_1$  minimization approach exhibits phase transition in the plane of  $(\delta, \rho)$ , and a larger  $N$  can result in sharper phase transition.
- II. the complex phase transition of  $\ell_1$  minimization is higher than the real phase transition with a considerably enlarged success phase.

**Finding 2:** For complex signals and the partial-Fourier matrix ensemble with large dimension  $N$ , the phase transition of the indirect method matches the real phase transition.

**Remark 1:** Finding 1 says that it is easier to reconstruct a complex signal than to reconstruct a real one in the sense that less samples are required. An intuitive interpretation of this finding is as follows. Suppose that there are  $k$  nonzero entries in the complex signal  $\mathbf{x}$ . We need to recover  $2k$  variables from  $2n$  samples when treating a complex number as two real numbers as in the indirect method. But a constraint is omitted in the indirect method that the  $2k$  nonzero entries are in fact  $k$  pairs while it is exploited in the ONE-L1 algorithms for  $(P_1)$  via jointly processing the real and imaginary parts.

TABLE I  
FAILURE NUMBERS AND CPU TIME CONSUMPTIONS IN THE ESTIMATION  
OF PHASE TRANSITIONS USING THE ONE-L1 ALGORITHMS

Ensemble	Dim. $N$	Method	Failure number			Time (hour)
			$\delta = 0.02$	$\delta = 0.05$	Others	
Fourier	1024	exact	0(480) <sup>1</sup>	0(340)	0(8180)	6.26
Fourier	1024	relaxed	14(440)	4(340)	0(8280)	0.327
Fourier	2048	relaxed	1(320)	1(320)	0(7460)	0.594
Fourier	4096	relaxed	4(240)	0(260)	0(6980)	1.01
Fourier	8192	relaxed	1(260)	0(240)	0(6660)	2.15
Fourier	1024	indirect	4(300)	1(260)	14(7400)	0.361
Gaussian	1000	relaxed	16(420)	0(340)	0(8240)	5.56
Bernoulli	1000	relaxed	9(420)	2(360)	0(8340)	5.60
Ternary	1000	relaxed	9(360)	2(280)	0(8240)	5.65

<sup>1</sup>In the brackets is the corresponding number of problem instances solved.

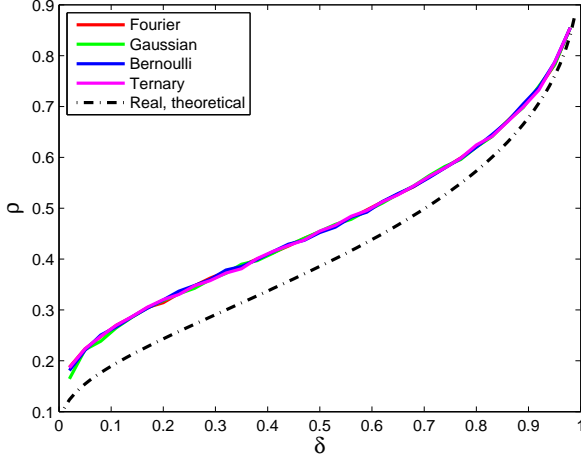


Fig. 3. Observed universality of phase transitions of  $(P_1)$  in the complex domain. The signal length  $N = 8192$  for partial-Fourier matrix ensemble and  $N = 1000$  for the other three matrix ensembles.

### C. Universality of Phase Transitions of Complex CS

The observed universality of phase transitions of  $(P_1)$  in the real case has been discussed in [11] and the same result is also stated in [10], [13]. In this subsection, we examine whether the same property holds in the complex case. Apart from the partial-Fourier matrix ensemble, three other complex matrix ensembles are considered with signal length  $N = 1000$ , including Gaussian, Bernoulli and Ternary. All random matrices have i.i.d. real and imaginary parts following the corresponding distributions. Bernoulli refers to equally likely being 0 or 1, and Ternary is equally likely to be  $-1, 0$  or  $1$ .

Few failures to solve  $(P_1)$  occur in our experiment, as shown in Table I. Fig. 3 presents the observed phase transitions of  $(P_1)$  with different matrix ensembles. Like the universality of phase transitions of  $(P_1)$  in the real case, we have the following finding.

**Finding 3:** For complex signals and a number of complex matrix ensembles with large dimension  $N$ , the  $\ell_1$  minimization approach exhibits the same phase transition.

## IV. CONCLUSION

In this letter, the sparsity-undersampling tradeoff of  $\ell_1$  minimization for the complex valued CS problem has been

empirically explored in terms of the phase transition. It has been found that the same properties exist as those in the real valued CS case, such as the existence of the phase transition and observed universality across different matrix ensembles. A remarkable discovery is that the complex phase transition is superior to that of the real valued CS, which provides a considerably enlarged success region in the phase plane. This indicates that, under the same signal sparsity, a success in reconstruction of complex sparse signals requires less number of samples than that required in the real valued CS.

A part of the results in this letter was earlier presented in a conference paper [16]. It is also noted that an analysis, based on a different algorithm, of the existence of the complex phase transition and its expression, which agrees with our results, have been reported in [17] during the preparation of this paper.

## REFERENCES

- [1] E. Candès, J. Romberg, and T. Tao, "Robust uncertainty principles: Exact signal reconstruction from highly incomplete frequency information," *IEEE Trans. Info. Theo.*, vol. 52, no. 2, pp. 489–509, 2006.
- [2] D. Donoho, "Compressed sensing," *IEEE Transactions on Information Theory*, vol. 52, no. 4, pp. 1289–1306, 2006.
- [3] E. Candès and J. Romberg, "Sparsity and incoherence in compressive sampling," *Inverse Problems*, vol. 23, pp. 969–985, 2007.
- [4] E. Candès, "The restricted isometry property and its implications for compressed sensing," *Comptes Rendus Mathematique*, vol. 346, no. 9–10, pp. 589–592, 2008.
- [5] D. Donoho and J. Tanner, "Counting the faces of randomly-projected hypercubes and orthants, with applications," *Discrete and Computational Geometry*, vol. 43, no. 3, pp. 522–541, 2010.
- [6] J. Blanchard, C. Cartis, and J. Tanner, "Compressed sensing: How sharp is the restricted isometry property," *arXiv:1004.5026*, 2010.
- [7] M. Lustig, D. Donoho, and J. Pauly, "Sparse MRI: The application of compressed sensing for rapid MR imaging," *Magnetic Resonance in Medicine*, vol. 58, no. 6, pp. 1182–1195, 2007.
- [8] M. Herman and T. Strohmer, "High-resolution radar via compressed sensing," *Signal Processing, IEEE Transactions on*, vol. 57, no. 6, pp. 2275–2284, 2009.
- [9] Z. Yang, L. Xie, and C. Zhang, "Off-grid direction of arrival estimation using sparse Bayesian inference," *arXiv:1108.5838*, 2011.
- [10] Z. Yang, C. Zhang, J. Deng, and W. Lu, "Orthonormal expansion  $\ell_1$ -minimization algorithms for compressed sensing," *arXiv:1108.5037*, to appear in *IEEE Trans. Sign. Proc.*, 2011.
- [11] D. Donoho and J. Tanner, "Observed universality of phase transitions in high-dimensional geometry, with implications for modern data analysis and signal processing," *Philosophical Transactions of the Royal Society A*, vol. 367, no. 1906, pp. 4273–4293, 2009.
- [12] M. Stojnic, "Various thresholds for  $\ell_1$ -optimization in compressed sensing," *arXiv:0907.3666*, 2009.
- [13] D. Donoho, A. Maleki, and A. Montanari, "Message-passing algorithms for compressed sensing," *Proceedings of the National Academy of Sciences*, vol. 106, no. 45, pp. 18914–18919, 2009.
- [14] G. Taubock and F. Hlawatsch, "A compressed sensing technique for OFDM channel estimation in mobile environments: Exploiting channel sparsity for reducing pilots," in *Acoustics, Speech and Signal Processing, IEEE International Conference on*. IEEE, 2008, pp. 2885–2888.
- [15] J. Picard and A. Weiss, "Direction finding of multiple emitters by spatial sparsity and linear programming," in *Proc. ISCIT 2009*. IEEE, pp. 1258–1262.
- [16] Z. Yang and C. Zhang, "Sparsity-undersampling tradeoff of compressed sensing in the complex domain," in *Proc. ICASSP*. IEEE, May 2011, pp. 3668–3671.
- [17] A. Maleki, L. Anitori, Z. Yang, and R. Baraniuk, "Asymptotic analysis of complex lasso via complex approximate message passing (camp)," *Arxiv preprint arXiv:1108.0477*, Aug. 2011.